An Iterative Solution of the Two-Dimensional Electromagnetic Inverse Scattering Problem*

Y. M. Wang and W. C. Chew

Electromagnetic Laboratory, Department of Electrical and Computer Engineering, University of Illinois, Urbana, Illinois 61801

A new method, based on an iterative procedure, for solving the two-dimensional inverse scattering problem is presented. This method employs an equivalent Neumann series solution in each iteration step. The purpose of the algorithm is to provide a general method to solve the two-dimensional imaging problem when the Born and the Rytov approximations break down. Numerical simulations were calculated for several cases where the conditions for the first order Born approximation were not satisfied. The results show that in both high and low frequency cases, good reconstructed profiles and smoothed versions of the original profiles can be obtained for smoothly varying permittivity profiles (lossless) and discontinuous profiles (lossless), respectively. A limited number of measurements around the object at a single frequency with four to eight plane incident waves from different directions are used. The method proposed in this article could easily be applied to the three-dimensional inverse scattering problem, if computational resources are available.

I. INTRODUCTION

It is well recognized that electromagnetic imaging has several potential advantages over other techniques. Of particular interest is the ability to image parameters such as dielectric constant and conductivity over a wide range of frequencies. It can provide additional information which could be complementary to that obtained by other imaging techniques. Furthermore, electromagnetic imaging is of interest to various disciplines such as medical imaging, geophysical explorations, remote sensing, and nondestructive testing.

In electromagnetic imaging, diffraction effects are important and cannot be neglected without decreasing the quality of the imaging. In weak scattering cases, the diffraction tomography (DT) approach has been introduced and investigated within the framework of the Born and the Rytov approximations [1–4], where the diffraction effects are supposed to be weak but not negligible. Unfortunately these conditions are not frequently satisfied in practical problems. The limitations of the Born and the Rytov approximations have been investigated by Keller [5], and Slaney, Kaki, and Larsen [6]. To consider the effects of strong diffraction, the nonlinear integral equation of inverse scattering problems has to be solved without the Born approximation.

Although intensive investigations are being undertaken on the inverse scattering theory, few solutions have been reported for the reconstruction of the dielectric distribution in higher dimensional cases in the literature. Wolf [7] proposed a method for reconstructing permittivity distributions of objects from their holograms taken at different angles of irradiation. Using the time domain analysis, Tijhuis [8] proposed an iterative technique for one-dimensional permittivity distribution reconstruction. An iterative procedure called the distorted Born approximation which is equivalent to the Newton iteration method had been proposed by Chew and Chuang [9] and Habashy, Chew, and Chow [10] for one-dimensional reconstruction of permittivity and conductivity distributions. Recently, a point matching method was used to reconstruct dielectric properties of a three-dimensional model of a human body within the framework of the first order approximations [11]. A method called pseudoinverse transformation [12] was proposed to reconstruct two-dimensional dielectric distributions. In this method, the current source is first reconstructed, and then the object is recovered from the current source. Consequently, the success of the method depends on the solution of the inverse source problem which faces the difficulties of nonuniqueness because of the existence of nonradiating sources [13–15]. A double iterative algorithm based on expansion of both ϵ_r and total electric field E was proposed to solve the two-dimensional inverse scattering problem by using sine basis functions and multiple source technique [16, 17]. However, the criteria for which the iteration algorithm will yield convergent solutions were not clearly mentioned.

In the present article, an iteration algorithm called the modified Newton method is being proposed to solve the two-dimensional electromagnetic nonlinear inverse scattering problem. The moment method has been employed to solve the forward scattered fields. A regularization method has been used in the inverse procedure to circumvent nonuniqueness and instability of the inverse solution. The examples given in this article show that the algorithm can be used to reconstruct the two-dimensional dielectric distributions in a wide range of situations where the Born approximation fails. In all examples, final convergent solutions are obtained after a few iterations—from five to twelve iterations.

*This work is supported by National Science Foundation under grant NSF ECS-85-25891, Office of Naval Research under grant N000-14-89-J1286, Schlumberger, and TRW.

Received March 3, 1989.
International Journal of Imaging Systems and Technology, Vol. 1, 100–108 (1989).

II. THEORY AND FORMULATION

The geometry of the two-dimensional inverse problem is shown in Figure 1. The cylindrical medium with an arbitrary cross section is inhomogeneous in the xy plane but is homogeneous in the z axis. The receivers are located around the cylindrical object at finite discrete points. The object is illuminated by either a plane wave or the field excited by an electrical current line source indicated as T in Figure 1. In the present article TM incident waves are supposed in both the plane wave and line source cases since the operator involved in the basic equation becomes much simpler for TM irradiation than that for TE irradiations [18] and, consequently, yields a better accuracy for a scattered field solution [19]. For pure TM incident waves, Maxwell's equations reduce to a scalar equation

$$\nabla_s^2 E_z(x, y) + k^2(x, y) E_z(x, y) = -i\omega\mu_0 J_z^i \qquad (1)$$

Here, a normal incident has been assumed, and

$$\nabla_s^2 \equiv \frac{\partial^2}{\partial x^2} + \frac{\partial^2}{\partial y^2}$$

$$k^2 = \omega^2 \mu_0 \epsilon(x, y)$$

Equation (1) can be cast into an integral equation as

$$E_z(x, y) = E_z^i(x, y) + \int\int_S G(\boldsymbol{\rho} - \boldsymbol{\rho}') \times k_0^2 \delta\epsilon_r E_z(x', y')\, dx'\, dy' \qquad (2)$$

where S is the scatterer cross section, and

$$G(\boldsymbol{\rho} - \boldsymbol{\rho}') = (i/4) H_0^{(1)}(k_0 |\boldsymbol{\rho} - \boldsymbol{\rho}'|) \qquad (3)$$

is the two-dimensional Green's function for a homogeneous medium, and

$$\delta\epsilon_r = \epsilon_r(x, y) - 1$$

is the permittivity profile to be recovered.

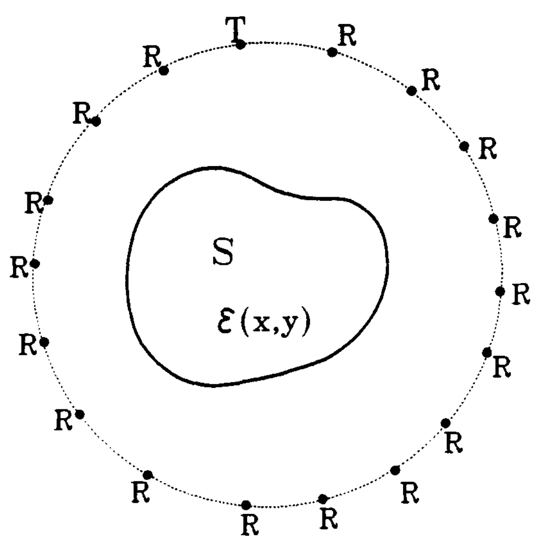

Figure 1. Geometrical configuration of the problem.

In weak scattering cases, where the scattered field is much smaller than the incident field, the integral equation (2) can be solved for $\delta\epsilon_r$ under the Born or Rytov approximations. Unfortunately, the distortions of the reconstructed profile become intolerable under the first approximation when the criteria are not satisfied. In these cases, the strong diffraction effects have to be considered, which means that the inherent nonlinearity of the integral equation (2) has to be taken into account. In this article, an iterative algorithm called the modified Newton method has been proposed to solve the integral equation (2) for $\delta\epsilon_r(x, y)$, in which the Green's function, $G(\boldsymbol{\rho} - \boldsymbol{\rho}')$, remains unchanged in the iteration procedures. The outline of this approach can be summarized in the following steps:

(1) Solve the linearized inverse problem for the first order distribution function by using the Born approximation.
(2) Solve the scattering problem for the field in the object and at the observation points with the last reconstructed distribution function.
(3) Substitute the field in the object obtained in step (2) into the integrand in the integral equation and solve the inverse problem to recover the next order distribution function.
(4) Repeat step (2) and compare the field obtained by the reconstructed distribution function and the measured data, which in our case are the simulated fields for the exact distribution function at the observation points. If the difference is less than 5% of the scattered field, the iteration terminates, otherwise repeat the cycle until the solution is convergent.

Notice that to implement this algorithm, both the forward and inverse solvers are needed. In this article, the point matching method with the pulse basis function has been employed to solve the forward scattering problem for the scattered field inside the object and at the observation points. More attention should be paid to the choice of the inverse procedure because of the inherent instability and nonuniqueness of the inverse scattering problem.

There are two things involved in solving the linearized version of the integral equation (2) for the permittivity profile solution in each iteration. In the first step, one must discretize the problem to reduce it to an approximate linear algebraic representation of the linearized version of integral equation (2). Here, the method of basis function expansion [20] has been employed. In this method, one needs to choose a set of basis functions $\{f_i(x, y)\}$ which could accurately represent the behavior of the expected permittivity profile. To simplify the numerical calculation and obtain the expected accuracy, we choose the pulse function as the basis functions which are the same as that we used in the moment method for solving the forward scattering problem. Using the pulse basis function $\{f_i(x, y)\}$, the unknown permittivity profile $\delta\epsilon_r(x, y)$ can be written as

$$\delta\epsilon_r(x, y) = \sum_{i=1}^{N} a_i f_i(x, y)\,, \quad x, y \in S \qquad (4)$$

Substituting equation (4) into the integral equation (2) and considering that the measured data are at the finite points around the object, we have

$$E_z^s(x_j, y_j) = \sum_{i=1}^{N} a_i \int\int_{S_i} G(\boldsymbol{\rho}_j - \boldsymbol{\rho}')k_0^2 f_i(x', y') \times E_z^{(r)}(x', y')\, dx'\, dy', \quad j = 1, \ldots, M \tag{5}$$

where S_i is the domain of the pulse function $f_i(x, y)$, and $E_z^{(r)}$ is the forward scattering solution of order r, when $r = 0$. It is the incident field in the object (the Born approximation). M in equation (5) is the number of the independent measurement data; in our case, it is the product of the number of receivers and the number of incident waves or transmitters. Equation (5) can be rewritten as a matrix equation

$$\mathbf{b} = \mathbf{K} \cdot \mathbf{a} \tag{6}$$

here

$$\mathbf{b} = [E_z^s(\boldsymbol{\rho}_1), E_z^s(\boldsymbol{\rho}_2), \ldots, E_z^s(\boldsymbol{\rho}_M)]^T$$
$$\mathbf{a} = (a_1, a_2, \ldots, a_N)^T$$

and $\mathbf{K}$ is a $M \times N$ matrix whose elements are

$$K_{ji} = \int\int_{S_i} k_0^2 G(\boldsymbol{\rho}_j - \boldsymbol{\rho}')E_z^{(r)}(x', y') f_i(x', y')\, dx'\, dy'$$
$$i = 1, \ldots, N, \; j = 1, \ldots, M$$

Since $E_z^{(r)}(x, y)$ is the solution of the forward problem and the same pulse functions are used in both the forward and inverse procedures, $E_z^{(r)}(x, y)$ can be approximately expressed as a constant in each patch. Hence, the above expression becomes

$$K_{ji} = k_0^2 E_z^{(r)}(\boldsymbol{\rho}_i) \int\int_{S_i} G(\boldsymbol{\rho}_j - \boldsymbol{\rho}')\, dx'\, dy'$$

where ρ_i is the coordinate of the center of patch i. Notice that the integration in the above equation is unchanged for every iteration. Thus it can be saved in a matrix for use later.

In the second step, one needs to solve the linear equation (6) for the coefficients of the permittivity profile expansion. It is a simple matter, in principle, to solve this system to yield a numerical approximation of the solution. On first sight, it appears that the system of equations in equation (6) provides a simple and robust numerical inversion technique for solving the linearized version of equation (2). In practice, however, this method faces a severe difficulty because of the ill-conditioned matrix $\mathbf{K}$ [20, 21]. The difficulty in the direct inversion method is clearly a consequence of the fact that the measured data cannot provide sufficient information on the high frequency components of the solution. In other words, the measured data imply only that the solution must lie in a specified class of the solutions, but they provide no guidance as to what unique choice is to be made within that class. Furthermore, evanescent waves scattered from the object become exponentially small at the receivers. They also exacerbate the ill conditioning of the problem. The key idea of the regularization is to impose an additional constraint on the linear system (6) which enables us to select one of the possible solutions [20, 21]. This constraint is arbitrary, in principle, and is not derived from measured data, but might be a priori information, i.e., the continuity of the distribution function. Although this additional constraint is arbitrary, it does provide us with an indirect way of selecting smooth profiles.

In the regularization procedure, instead of solving equation (6) for a least square solution, one solves

$$\|\mathbf{K} \cdot \mathbf{a} - \mathbf{b}\|^2 + \gamma \|\mathbf{H} \cdot \mathbf{a}\|^2 = min \tag{7}$$

where γ is the regularization parameter, and $\mathbf{H}$ is the smoothing matrix which is a matrix representation of the regularization functional operator. From equation (7), one obtains the following matrix equation:

$$[\mathbf{K}^\dagger \cdot \mathbf{K} + \gamma \mathbf{H}^\dagger \cdot \mathbf{H}] \cdot \mathbf{a} = \mathbf{K}^\dagger \cdot \mathbf{b} \tag{8}$$

where $\mathbf{K}^\dagger$ and $\mathbf{H}^\dagger$ are the conjugate transpose of $\mathbf{K}$ and $\mathbf{H}$, respectively. In this article, the zeroth-order regularization, in which $\mathbf{H}$ is the identity matrix of order N, has been used to generate results given in the next section. The solution of equation (8) is given by

$$\mathbf{a} = [\mathbf{K}^\dagger \cdot \mathbf{K} + \gamma \mathbf{H}^\dagger \cdot \mathbf{H}]^{-1} \cdot \mathbf{K}^\dagger \cdot \mathbf{b} \tag{9}$$

The choice of the arbitrary parameter γ is important in the regularization procedure. It must be properly balanced so that it is big enough to filter out unstable high frequency components to obtain a stable solution, but not too big so as to filter out too many useful frequency components in the solution. Generally speaking, however, there is no universal strategy for selecting the optimum γ, and it is probably best to regard γ as effectively undefined in any specific case. A safer approach is probably to base the selection of γ on the numerical simulations.

In practice, the range of γ over which the stable solution could be obtained also plays an important role in the inverse procedure. If the solution is too sensitive to the parameter γ, i.e., the range of γ which gives the stable solution is too small, for instance less than one order, then the problem may not be properly defined for the inverse solution because the information contained in the data is not enough to recover the profile with the expected accuracy. According to our experience, for a robust inversion algorithm, the range of γ which gives the stable solution should, at least, be three to five orders of magnitude, for example from 10^{-10} to 10^{-15}. One practical point that should be mentioned is that to have a convergent solution using the iterative procedure proposed in this article, one must have a suitable and robust standard inverse algorithm which has to pass the test by using numerical simulations in which the first order Born approximation is valid.

III. SIMULATIONS AND RESULTS

In this section, some simulated results are obtained for several cases from low frequency to high frequency electromagnetic images. Figure 2 shows the relative dielectric distribution reconstruction of a sinelike function with a peak value of 11. The frequency of the incident wave is 10 MHz. The diameter of the object is about one-tenth of the wavelength. Four incident plane waves from the different directions are illuminated in this and following examples except in the examples given in Figures 3 and 4 in which eight incident plane waves are illuminated. Receivers are located around the object as

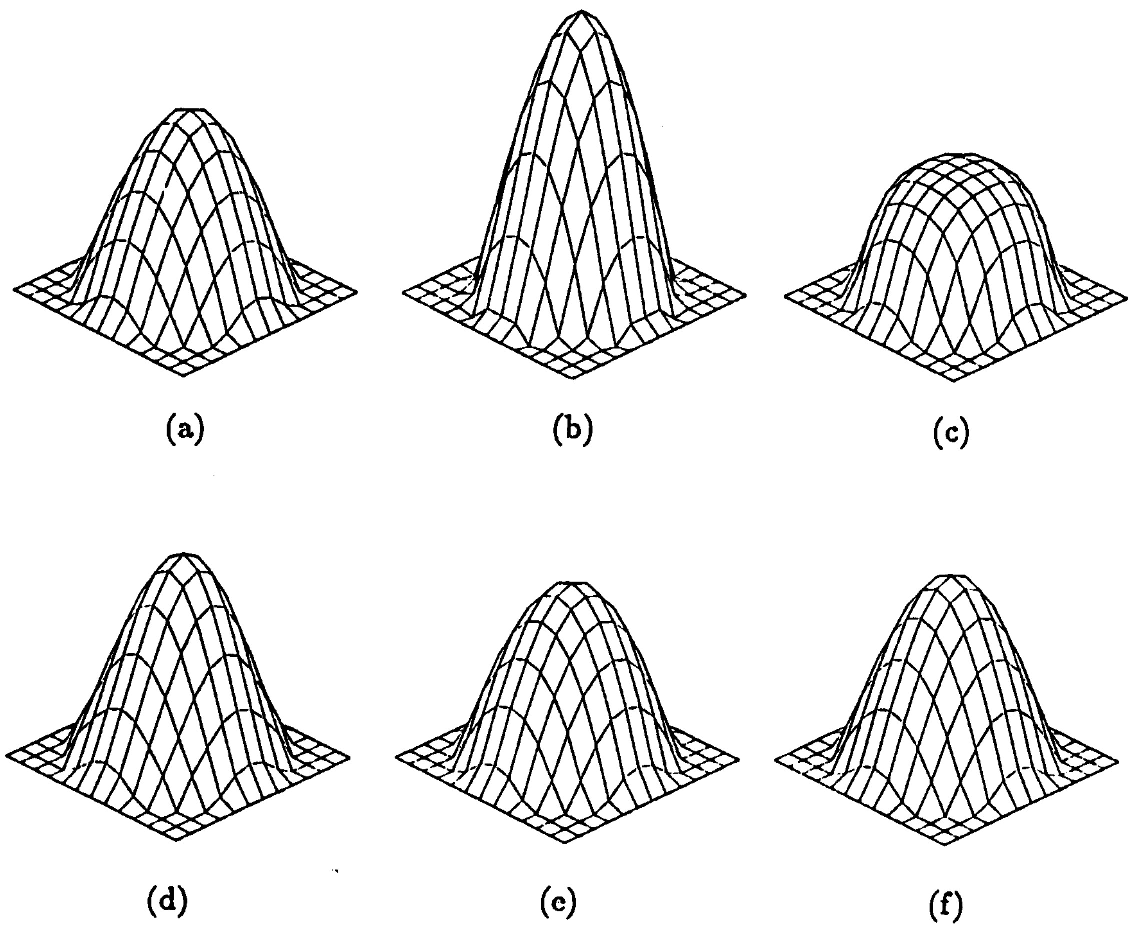

Figure 2. Reconstruction of a sinlike permittivity distribution with operating frequency at 10 MHz. The peak value of the relative permittivity is 11. The diameter of the object is one-tenth of the wavelength. (a) is the original distribution, (b) is the result of the first order approximation, (c)–(e) are the results from the second iteration to the fourth iteration, and (f) is the final convergent solution after five iterations.

indicated in Figure 1. The number of receivers in this and the following examples varies from 26 to 36 depending on the number of unknowns of the problem. The total number of the independent measurement which is the product of the number of incident waves and the number of the receivers will be from 104 to 288 for the examples in this section. The number of unknowns of the examples given in this section is the number of the grid points in the example which varies from 121 to 361 depending on the size of the scatterer. The measured data for all the examples in this section were simulated on the computer by solving the forward scattering problem with the original dielectric distribution functions for the scattered fields at the receivers.

Figure 2 shows clearly the evolution of the convergence of the solution given by the algorithm proposed in the article. Figure 2(a) is the original dielectric distribution function and Figure 2(b) is the reconstructed result of the first order approximation, i.e., the Born approximation. Here, we can see that the Born approximation fails for the quantitative reconstruction of the dielectric distribution function in this case. Figures 2(c) to 2(f) are iteration results from the second iteration to the fifth iteration. The solution converges to the original dielectric distribution function after five iterations. The above example shows that the algorithm works very well even when the Born approximation fails to reconstruct the distribution function in the low frequency inverse scattering problem.

Figure 3 shows the dielectric distribution reconstruction of a sinelike function with the operating frequency at 100 MHz. The peak value of the relative dielectric constant in the object is 1.80. The diameter of the object in this case is about 1λ. Figure 3(a) is the original dielectric distribution and Figure 3(b) is the reconstructed dielectric distribution of the first iteration, i.e., the Born approximation. Figures 3(c) to 3(h) are the iteration results from the second iteration to the seventh iteration. Figure 3(i) is the final convergent solution after eight iterations.

All simulation results given in this section are obtained on the SUN 4/110 workstation by using double precision. As is well known, to guarantee the accuracy of the calculated scattered field by using the moment method, the mesh density has to be about $100/\lambda^2$ [19]. Due to the limitation of the memory provided by the SUN workstation, the maximum size of the object we can deal with on the SUN is about 2λ in the dimension of the diameter. In Figure 4, the operating frequency is 200 MHz. The diameter of the object is about 2λ. In this example, eight plane waves are illuminated from the different directions. Figure 4(a) is the original dielectric distri-

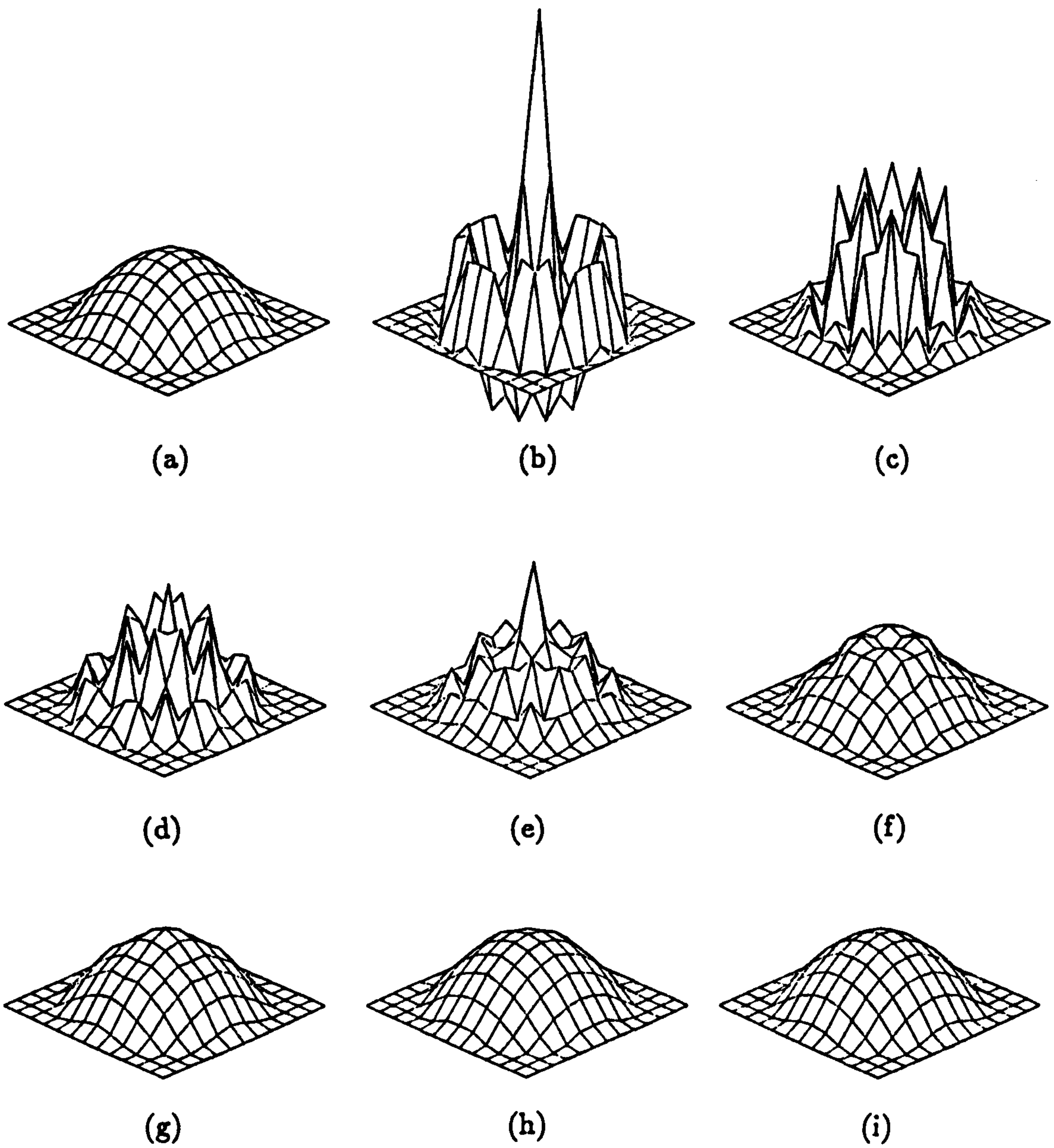

Figure 3. Reconstruction of a sinlike permittivity distribution with operating frequency at 100 MHz. The peak value of the relative permittivity is 1.80. The diameter of the object is one wavelength. (a) is the original distribution, (b) is the result of the first order approximation, (c)–(h) are the results from the second iteration to the seventh iteration, and (i) is the final convergent solution after eight iterations.

bution, Figure 4(b) is the reconstructed distribution of the first iteration and Figure 4(c) is the convergent solution of the dielectric distribution function after twelve iterations.

Some common features appear in all the examples given above. First, the Born approximation fails to give a quantitative reconstruction of the dielectric distribution in all the examples. Second, the final convergent solutions obtained by the algorithm proposed in the article converge to the exact distribution functions after a few iterations with the negligible errors, less than 1% at grid points. The reason for the high accuracy of the reconstructed dielectric distributions in the above examples is that the property of the constraint we employed in the inverse procedure coincides with that of the original distribution functions, i.e., continuity of the distribution functions. In the next two examples, the dielectric distribution functions with a discontinuity, i.e., step function, are considered. The result will give us an idea on how the algorithm works and what we can expect for a discontinuous distribution function.

Figure 5 shows the dielectric distribution reconstruction of a step function to illustrate the band-limited nature of the algorithm. The regularization employed in the inverse procedure causes the algorithm to exhibit some low-pass-filtering effect. As we see from Figure 5, the final convergent solution is, as we expected, a smoothed version of the original distribution function. In Figure 5, the operating frequency is 100 MHz. The diameter of the object is about one wavelength and $\delta\epsilon_r$ is 0.60. Figure 5(a) gives the original dielectric distri-

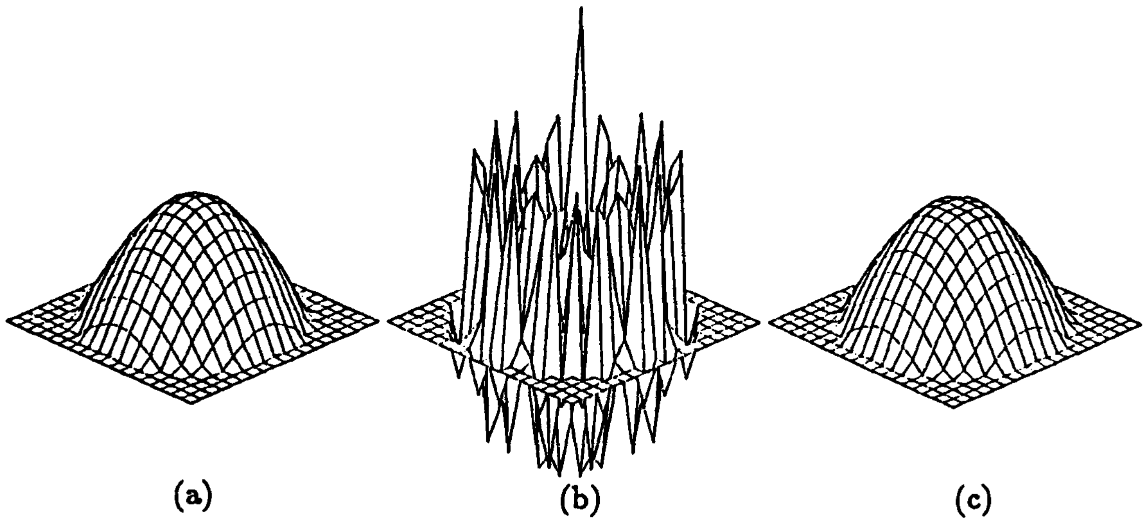

Figure 4. Reconstruction of a sinlike permittivity distribution with operating frequency at 200 MHz. The peak value of the relative permittivity is 1.80. The diameter of the object is 2λ. (a) is the original distribution, (b) is the result of the first order approximation, and (c) is the final convergent solution after 12 iterations.

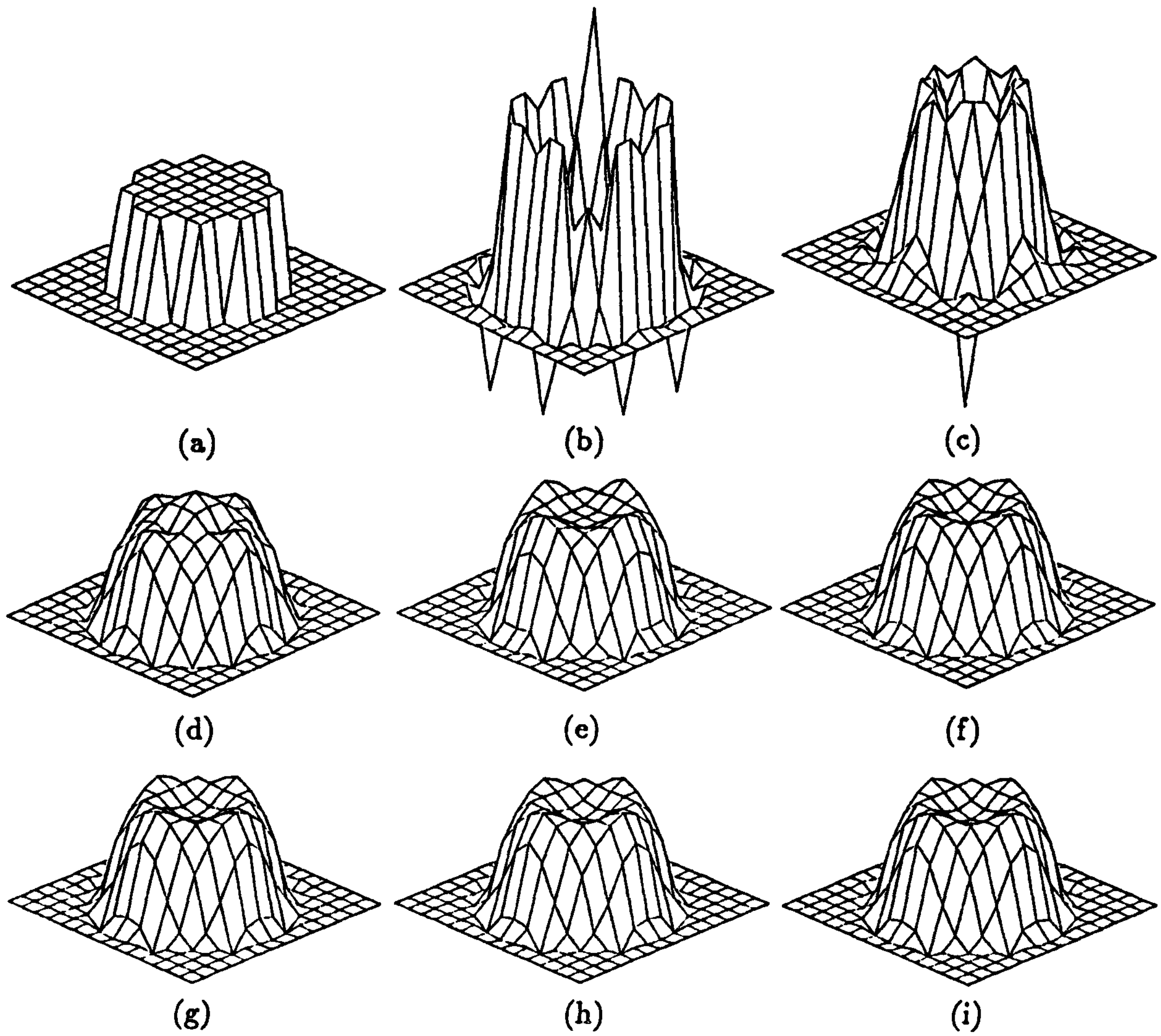

Figure 5. Reconstruction of a step permittivity distribution with operating frequency at 100 MHz. The contrast of the relative permittivity is 1:1.60. The diameter of the object is one wavelength. (a) is the original distribution, (b) is the result of the first order approximation, (c)–(h) are the results from the second iteration to the seventh iteration, and (i) is the final convergent solution after eight iterations.

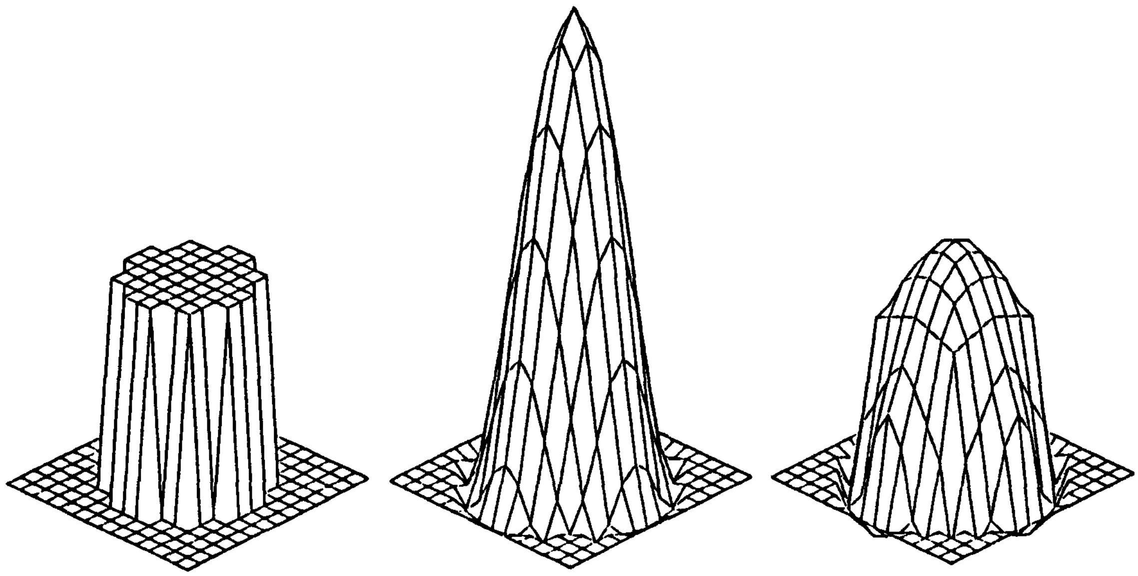

(a) (b) (c)

Figure 6. Reconstruction of a step permittivity distribution with operating frequency at 10 MHz. The contrast of the relative permittivity is 1 : 11. The diameter of the object is one-tenth of the wavelength. (a) is the original distribution, (b) is the result of the first order approximation, and (c) is the final convergent solution after five iterations.

bution, Figure 5(b) is the result of the first iteration, i.e., the Born approximation, and Figures 5(c) to 5(i) are the results from the second iteration to the eight iteration, respectively. The solution converges after eight iterations.

Figure 6 shows the similar behavior as that in Figure 5. But in this example, the operating frequency is 10 MHz. The diameter of the object is about one-tenth of the wavelength and $\delta\epsilon_r$ is 10. Figure 6(a) gives the original dielectric distribution, Figure 6(b) gives the result of the first iteration, and Figure 6(c) is the final convergent solution after five iterations.

As the last example, Figure 7 shows that the convergent solution of the reconstruction of an asymmetric dielectric distribution agrees quite well with the original one. Figure 7(a) is the original dielectric distribution, and Figure 7(b) is the convergent solution of the constructed distribution after six iterations. However, because of the band-limited nature of the algorithm, computation shows that high spectral frequency components of the distribution function were smoothed out.

Figure 8 gives the relative mean squared error (MSE) of the reconstructed permittivity distribution in Figure 3 as a function of the iteration steps. The relative MSE is defined as

$$\mathrm{MSE} = \sqrt{\frac{\int\int_S [\epsilon_r^{(i)}(\boldsymbol{\rho}) - \epsilon_r(\boldsymbol{\rho})]^2 \, dx\, dy}{\int\int_S [\epsilon_r(\boldsymbol{\rho})]^2 \, dx\, dy}} \tag{9}$$

where S is the scatterer cross section, $\epsilon_r^{(i)}(\boldsymbol{\rho})$ is the ith iterative reconstructed relative permittivity distribution, and $\epsilon_r(\boldsymbol{\rho})$ is the original relative permittivity distribution.

The numerical simulations we did in this section covered a wide range of the electromagnetic inverse scattering applications, from low frequency with high contrast cases to high frequency with moderate contrast cases. According to the

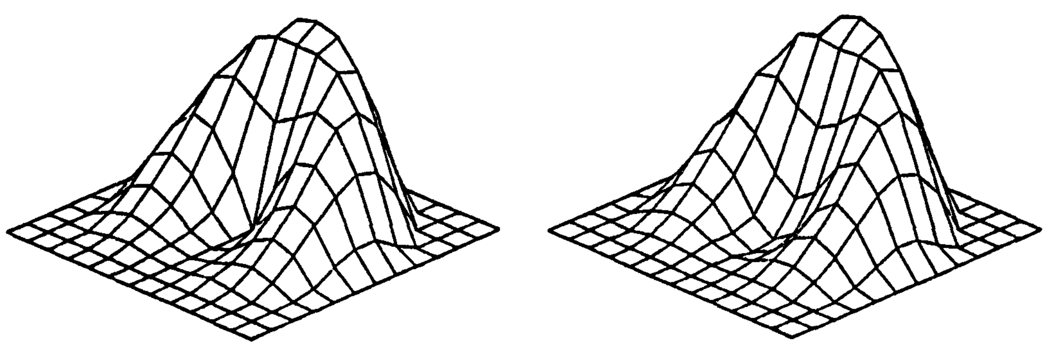

(a) (b)

Figure 7. Reconstruction of an axially asymmetric permittivity distribution with operating frequency at 100 MHz. The peak value of the relative permittivity is 1.80. The diameter of the object is one wavelength. (a) is the original distribution and (b) is the final convergent solution after six iterations.

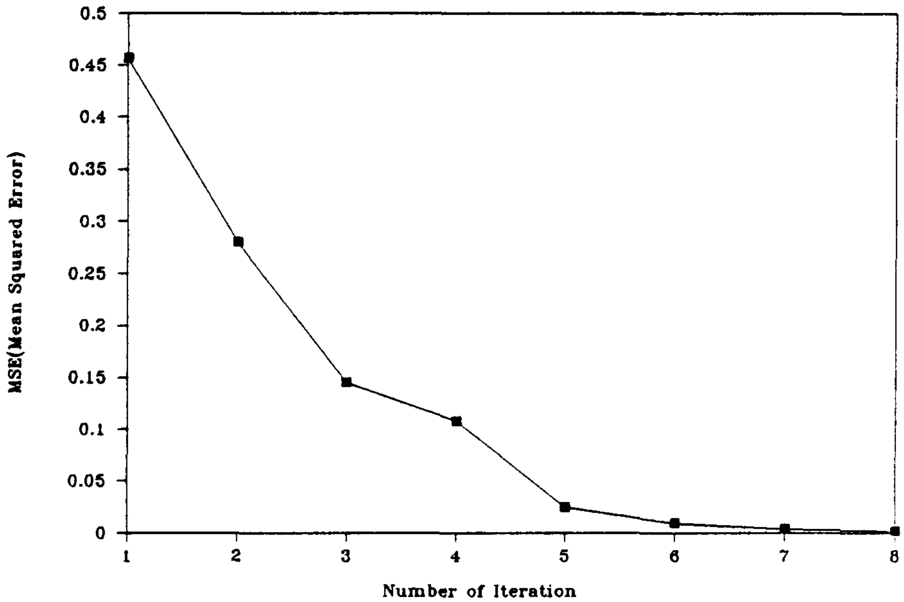

Figure 8. The relative MSE of the reconstructed permittivity distribution in Figure 3 as a function of the iteration steps.

results of the numerical simulations, we conclude that the algorithm can be successfully applied to the reconstruction of the dielectric distribution when the first order Born approximation fails for the quantitative reconstruction. The simulations established that the maximum contrast of the relative dielectric constant, in which the algorithm gives correct convergent solution, is ten times more than that for the Born approximation at the fixed frequency.

CONCLUSIONS

An algorithm for solving two-dimensional electromagnetic nonlinear inverse scattering problems has been proposed. The algorithm has been successfully applied to the reconstruction of the dielectric distribution functions in a wide range of situations where the Born approximation fails. It turns out, according to the results of the numerical simulations, that the maximum contrast of the dielectric constant can be relaxed by a factor of ten compared to that for the Born approximation. The relaxation of the criteria is important in many areas of the inverse scattering applications such as medical imaging, nondestructive testing, and geophysical explorations.

It is very important to note that the algorithm proposed in this article could be implemented easily in the framework of the existing diffraction tomography (DT) by adding a suitable forward scattering solver and an iterative procedure because the problem has been linearized in each iteration step. The combination of the algorithm and conventional diffraction tomography provides a potential method to implement nonlinear diffraction tomography in the real world of applications.

REFERENCES

[1] A. J. Devaney, A computer simulation study of diffraction tomography, *IEEE Trans. Biomed. Eng.*, **30**, 377–386 (1983).

[2] M. Azimi and A. C. Kak, Distortion in diffraction tomography caused by multiple scattering, *IEEE Trans. Med. Imaging*, **2**, 176–195 (1983).

[3] W. Tabbara, B. Duchêne, Ch. Pichot, D. Lesselier, L. Chommeloux, and N. Joachimowicz, Diffraction tomography: contribution to the analysis of applications in microwaves and ultrasonics, *Inverse Problem*, **4**, 305–331 (1988).

[4] A. J. Devaney, A filtered backpropagation algorithm for diffraction tomography, *Ultrasonic Imaging*, **4**, 336–360 (1982).

[5] J. B. Keller, Accuracy and validity of the Born and Rytov approximations, *J. Opt. Soc. Am.*, **59**, 1003–1004 (1969).

[6] M. Slaney, A. C. Kak, and L. E. Larsen, Limitations of imaging with first-order diffraction tomography, *IEEE Trans. Microwave theory and Techniques*, **32**, 860–874 (1984).

[7] E. Wolf, Three-dimensional structure determination of semi-transparent objects from holographic data, *Opt. Commun.* **1**, 153–169 (1969).

[8] A. J. Tijhuis, Iterative determination of permittivity and conductivity profiles of a dielectric slab in time domain, *IEEE Trans. Antennas Propag.*, **29**, 239–245 (1981).

[9] W. C. Chew and S. L. Chuang, *Profile inversion of a planar medium with a line source or a point source*, paper presented at International Geoscience and Remote Sensing Symposium, Strasbourg, France, 1984.

[10] T. M. Habashy, W. C. Chew and E. Y. Chow, Simultaneous reconstruction of permittivity and conductivity profiles in a radially inhomogeneous slab, *Radio Science*, **21**, 635–645 (1986).

[11] D. K. Ghodgonkar, O. P. Gandhi, and M. J. Hagmann, Estimation of complex permittivities of three-dimensional inhomogeneous biological bodies, *IEEE Trans. Microwave Theory Tech.*, **31**, 442–446 (1983).

[12] M. M. Ney, A. M. Smith, S. S. Stuchly, A solution of electromagnetic imaging using pseudoinverse transformation, *IEEE Trans. Medical Imaging*, **3**, 155–162 (1984).

[13] N. Bleistein and J. K. Cohen, Nonuniqueness in the inverse source problem in acoustics and electromagnetics, *J. Math. Phys.*, **18**, 194–201 (1977).

[14] A. J. Devaney and G. C. Sherman, Nonuniqueness in inverse source and scattering problems, *IEEE Trans. Ant. Propagation*, **8**, 1034–1042 (1982).

[15] A. J. Devaney and E. Wolf, Radiating and nonradiating classical

current distributions and the fields they generate, *Phys. Rev. D*, **8**, 1044–1047 (1973).
[16] S. J. Johnson and M. L. Tracy, Inverse scattering solutions by a sinc basis, multiple source, moment method—part I: theory, *Ultrasonic Imaging* **5**, 361–375 (1983).
[17] S. J. Johnson and M. L. Tracy, Inverse scattering solutions by a sinc basis, multiple source, moment method—part II: numerical evaluations, *Ultrasonic Imaging*, **5**, 376–392 (1983).
[18] J. Richmond, Scattering by a dielectric cylinder of arbitrary crosssectional shape, *IEEE Trans. Antennas propagation*, **13**, 334–341 (1965).
[19] R. F. Harrington, *Field Computation by Moment Methods*. Krieger Publishing, Florida, 1983.
[20] S. Twomey, *Introduction to the Mathematics of Inversion in Remote Sensing and Indirect Measurements*, Elsevier Scientific, New York, 1977.
[21] C. T. H. Baker, *The Numerical Treatment of Integral Equations*, Clarenda, Oxford, 1977.